

EXPERIMENTAL STUDY FOR BEHAVIOR OF MICROPILE FOUNDATION

YOSHINORI NAKATA ¹ and TAKAHIRO KISHISHITA ²

¹Engineering Division, Kyokuto Corporation

²Technical Research Institute, Fujita Corporation

SUMMARY

JAMP (Japanese Association of Micropile) have conducted field tests for Micropile system to confirm feasibility and efficiency of micropile system for seismic retrofit of foundations in Japan. This paper presents the results of these studies. The behavior of micropile driven in the test filld is discussed based on the test results.

1. INTRODUCTION

After Kobe Earthquake, many seismic retrofit programs for bridge superstructures and substructures have been conducted in Japan. However, very few foundations have been retrofitted for following reasons;

- 1) Construction space for pile driving machine is not enough in many cases
- 2) Seismic resistance of retrofitted foundations is not clear
- 3) Foundation retrofit is costly

Micropile is "drilled and grouted pile" with steel pipes which diameters is less than 300mm and driven by boring machine, featuring small diameter with thick wall and mechanical joints with couplers not welding (Fig.1). The advantages of this system are practicable with small space, cost effective and less construction noise and vibration. Laboratory tests and field tests were conducted for confirmation of feasibility and efficiency of Micropile system for seismic retrofit of structural foundation. This article presents the outline of the tests and discusses the test results.

Micropile system is widely used for structural foundation and soil reinforcement in Europe and for some bridge retrofit project in the USA.

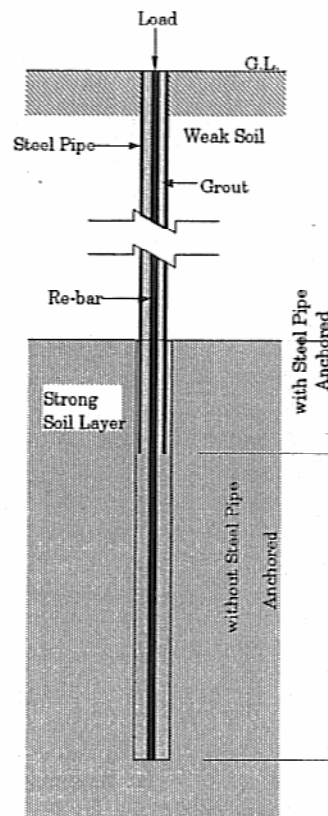


Fig. 1 Micropile System

2. OUTLINE OF TEST SETUP AND PROCEDURE

(1) Field tests of vertical compression loading and alternating vertical loading

Field tests of vertical compression loading (Fig.2) and alternating vertical loading (Fig.3) were performed for micropiles placed through a soft silt layer and supported on a hardpan layer, in order to

assess the structural strength of anchorage zones of micropiles, and the ultimate skin friction stress working between the grouting material and ground in a vicinity of the anchorage zones of steel pipes. Table 1 and Fig.4 show the specifications of the placed micropiles and the test apparatus, respectively. On the test piles, strain gauges were attached around the steel pipes and thread-lugged bars as shown in the figure, so as to enable confirmation of axial force distribution at different depths.

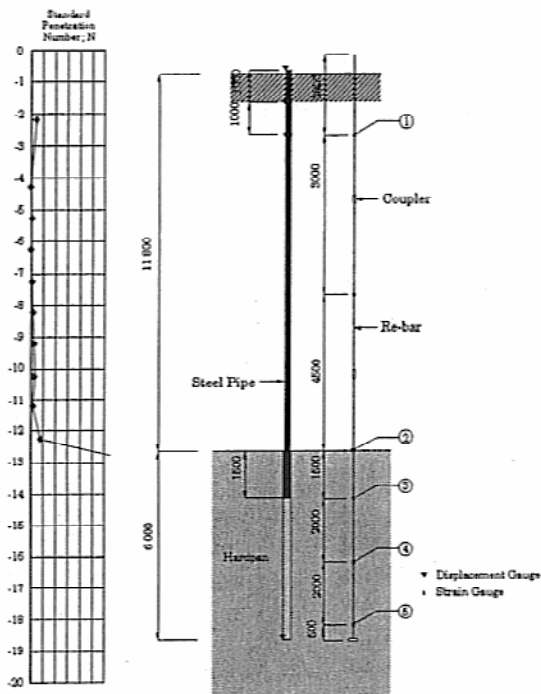


Fig. 2 Properties of soil and test piles

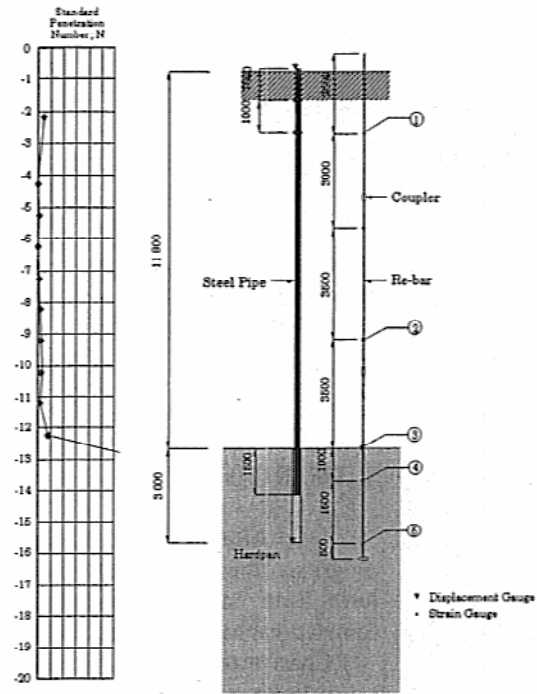


Fig. 3 Properties of soil and test piles

Table 1 Properties of test piles

Type of Testing	Vertical Loading Test
O.D./Thickness	177.8mm/12.7mm
Re-bar	SD490, D51
Compressive Strength of Grout	>35Nmm ² (W/C=45%)
O.D. of Anchorage Zone	φ 200mm

The maximum load applied for the vertical compression loading test was 3,600 kN, and loading was performed for 6 cycles in order to confirm the ultimate load. Strain gauges were attached on the reinforcement and steel pipes (Fig.2), in order to confirm axial force distribution at different depths.

In the alternating vertical loading tests, 4 cycles of compression and pull-out loads were applied alternately up to 800 kN using the loading apparatus shown in Fig.4. Then, after reaching the ultimate pull-out resistance, the load was increased further up to the ultimate load on the compression side.

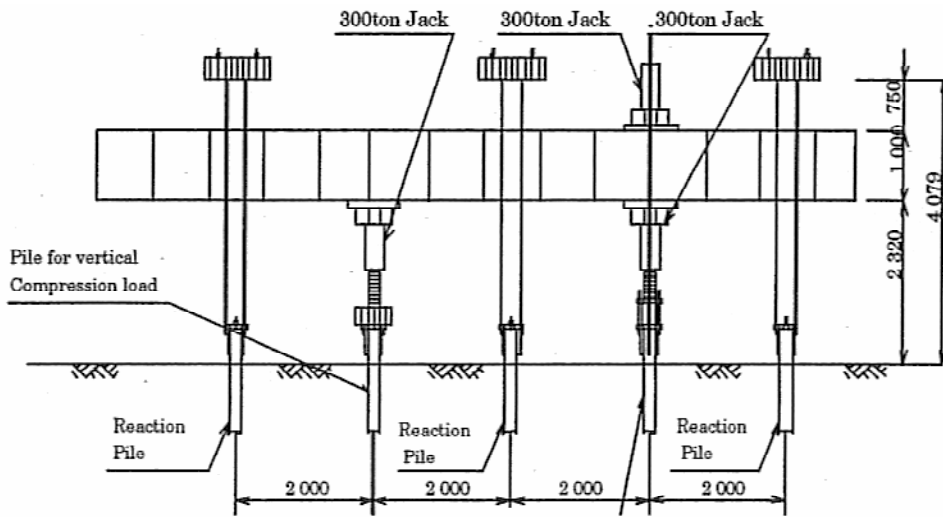


Fig. 4 Test setup

3. RESEARCH FINDINGS AND DISCUSSION

(1) Field tests of vertical compression loading

Fig.5 shows envelopes for the load-settlement relationship measured at pile ends and tips. Settlement at pile ends were small for loads up to 3,200 kN, and settlement characteristics were those caused mainly by elastic deformation. The most of the settlement is believed to be resisted by skin friction at anchorage zones. On the other hand, the majority of approximately 30 mm of settlement at pile ends are believed to be caused by compression. Since the ultimate strength of piles was about 3,300 kN, they are believed to have failed while the load was increased from 3,200 kN to 3,400 kN due to compression failure of grouting materials. This was confirmed by the fact that the pile ends settled by loading thereafter rapidly to 55 mm, while the pile tips settled for a very small amount of 5 mm.

Fig.6 shows strain distribution of measurements obtained by strain gauges attached to reinforcing bars and steel pipes. Strain of reinforcing bars within the anchorage zone of non-steel pipe exceeded 2,600 μ . Considering that stress at the yield point of reinforcement used was 522 N/mm², it is likely that the reinforcement yielded and grouting material failed due to compression. The unconfined axial strength of grouting material on the day of the test was about 52 N/mm².

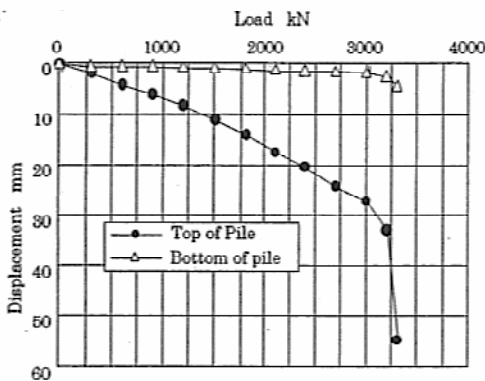


Fig.5 Load-displacement relationship

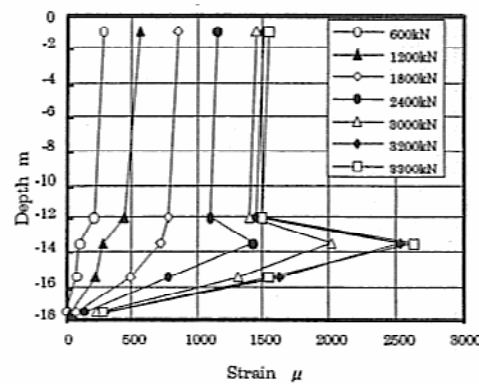


Fig.6 Strain distribution

Fig.7 shows axial strength distribution of the piles, calculated from the values of strain. The axial strength lowered drastically for depths below 12 m, indicating significant effect of skin friction at anchorage zones. Upon calculation of axial strength from the strain, the modulus of elasticity for both the steel pipes and reinforcement was assumed to be $2.0 \times 10^5 \text{ N/mm}^2$, and that for the grouting material to be $2.0 \times 10^4 \text{ N/mm}^2$, based on the results of unconfined compression tests on test pieces of the grouting material.

Fig.8 shows the relationship between the skin friction stress exerted between the grouting material and ground and relative displacement at the interface. The skin friction stress was derived based on the axial strength, assuming the effective diameter f of anchorage zone to be 200 mm. In the sections between the specimens Nos. 2 and 3 and Nos. 4 and 5, which consist largely of hardpan, the skin friction stress reached the maximum value for relative displacement between 4 and 8 mm, and decreased after the displacement reached 10 mm. On the other hand, skin friction stress in the section between the specimens Nos. 3 and 4 consisting mainly of fine sand increased along with the displacement, reaching 0.8 N/mm^2 at displacement of about 12 mm. Triaxial compression tests for the hardpan layer, or the supporting layer, showed its cohesion c to be 0.9 N/mm^2 , indicating that the results of tests performed for this study correspond well with information obtained pertaining to the ground anchor method.

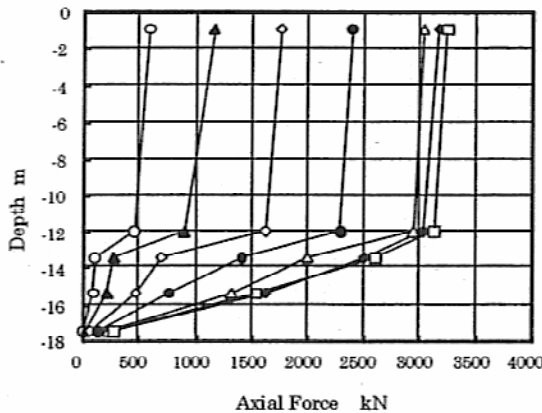


Fig.7 Axial force distribution

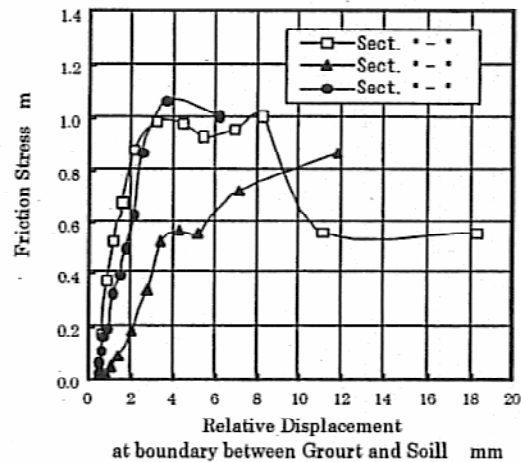


Fig.8 relationship between relative displacement and skin friction

(2) Field tests of alternating vertical loading

Fig.9 shows the load-enveloped displacement relationship under alternating loads and the load-displacement relationship until reaching the ultimate bearing capacity, both as continuous curves. Under the alternating loads up to 800 kN, displacements at pile ends and tips both shifted while maintaining linear relations with the loads. Thereafter, the ultimate bearing capacity for the pile ends and tips were reached at 1,050 kN and 1,700 kN respectively, under monotonous loading of either pull-out or compression force. As shown, the test results indicated that micropiles subjected to hysteretic pull-out forces maintain design bearing capacity to withstand repeated compression force, thus confirming that they function effectively under ultimate cyclic loads.

On the other hand, deformation of the pile body showed slight non-linearity after loading 1,200 kN of compression force. It was surmised that partial break in bonding between the reinforcement and grouting material caused by pull-out, as well as non-linear strength characteristics of the grouting material, brought about lowering of the pile body stiffness. Furthermore, measured values of distortion fluctuated after the compression load reached the above mentioned value, indicating a sign of deterioration in the pile body integrity.

Fig.10 shows axial strength distribution of the pile body estimated based on the strain values, for each step of loading. As shown, frictional resistance of the soft ground (at measuring points ① through ③) was minimal both under the compression and pull-out forces. As such, it was clear that the bearing

capacity of test piles depends on frictional resistance at anchorage zones formed within the hardpan layer. Skin friction stress conditions shown in Fig.11 and 12 reveal that skin friction at embedded section of steel pipes (measuring points ③ and ④) reached greater values during initial loading for both the compression and pull-out forces, and that the load is conveyed mostly by frictional resistance within the section. As the load increased, the friction distribution shifted to cover the tip of the anchorage zone. However, the skin friction stress at the embedded section of steel pipes continued to increase linearly until the ultimate state was reached.

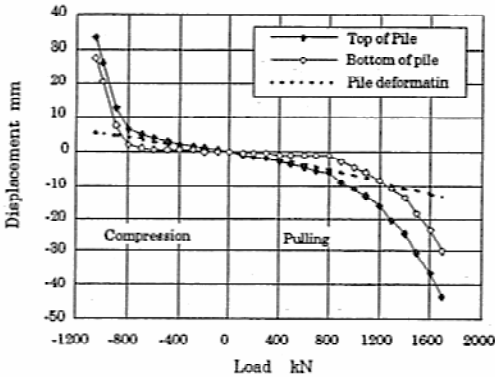


Fig.9 Load-displacement relationship

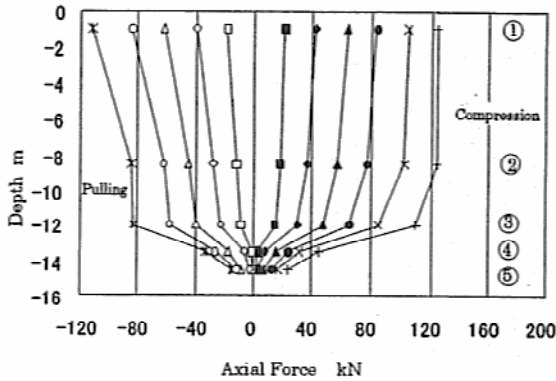


Fig.10 Axial force distribution

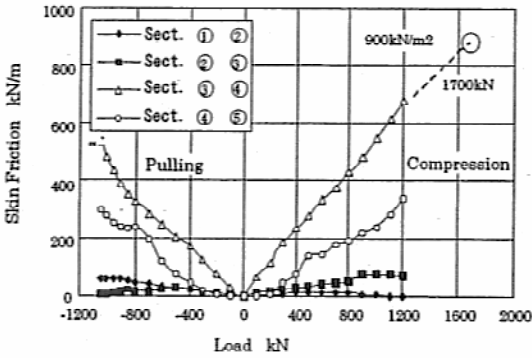


Fig.11 Relationship between load and skin friction

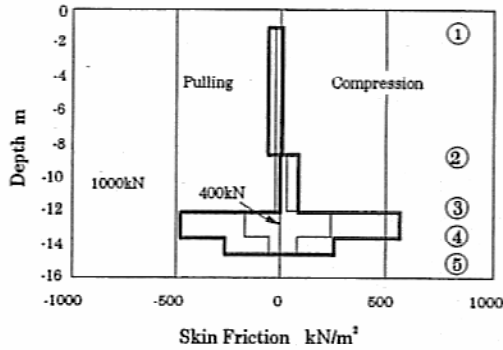


Fig.12 Skin friction distribution

On the other hand, the skin friction stress that reached the maximum value of 540 kN/m² under pull-out loads increased further under compression loads. Judging from the stress generated under loads up to 1,200 kN, it was surmised that the actual maximum value would be about 900 kN/m². This value is equivalent to that confirmed by vertical loading tests conducted under the same ground conditions. The differences in skin friction characteristics observed for different loading directions may be attributed to lateral deformation of the pile body and break in the bond between reinforcement and grouting material. The results of loading tests conducted for the study, however, have not yet clarified this issue.

4. CONCLUSION

The following information was obtained through the tests conducted for the study.

- 1) The ultimate compression bearing capacity of a micropile having 6-m long anchorage length supported

on a hardpan layer with q_u of about 2 N/mm^2 was 3,300 kN.

- 2) The pile failed when the reinforcement in anchorage zone of a non-steel pipe yielded and grouting material ruptured due to compression force.
- 3) The ultimate skin friction stress in the hardpan layer was approximately 1.0 kN/mm^2 . For cohesive soil, the value may be obtained assuming that f_u (the ultimate skin friction stress) equals the cohesion of the soil, as is in cases with ground anchor methods.
- 4) In some cases the strength of micropiles reinforced with steel pipes is governed by the compression strength of anchorage zone of a non-steel pipe. In such cases, the skin frictional resistance of the steel pipe anchorage zone may be added as compression strength of the pile body.
- 5) Compression strength of non-steel pipe anchorage zone is governed by the stress at yield point of reinforcing bars (if SD 490 is used). At this time, the portion of a load borne by the grouting material is estimated as 50 N/mm^2 in terms of stress, which was almost equal to the unconfined compression strength of 52 N/mm^2 obtained for test pieces of the grouting material.
- 6) Micropiles that were subjected to hysteretic pull-out loading maintained high bearing capacity to withstand compression load applied thereafter.
- 7) Distribution of skin friction at anchorage zones showed the greatest values at embedded section of steel pipes, both under the compression and pull-out forces. The ultimate skin friction stress under pull-out force was about $2/3$ of that under compression force.

With respect to bending properties of buried micropiles, it is necessary to accumulate data obtained from field horizontal loading tests, etc., in order to clarify interactions between the modulus of subgrade reaction and bending stiffness of the pile body. It should also be noted that data on bearing capacities obtained in the study may differ if the ground properties around anchorage zones and construction situations differ. Thus, it is necessary to conduct similar tests under various conditions in order to accumulate relevant data for establishment of calculation methods for bearing capacity and determination of safety factors.